Adipose Overexpression of Desnutrin Promotes Fatty Acid Use and Attenuates Diet-Induced Obesity

Maryam Ahmadian,[1] Robin E. Duncan,[1] Krista A. Varady,[1] Danubia Frasson,[1] Marc K. Hellerstein,[1] Andreas L. Birkenfeld,[2] Varman T. Samuel,[2] Gerald I. Shulman,[2] Yuhui Wang,[1] Chulho Kang,[3] and Hei Sook Sul[1]

OBJECTIVE—To investigate the role of desnutrin in adipose tissue triacylglycerol (TAG) and fatty acid metabolism.

RESEARCH DESIGN AND METHODS—We generated transgenic mice overexpressing desnutrin (also called adipose triglyceride lipase [ATGL]) in adipocytes (aP2-desnutrin) and also performed adenoviral-mediated overexpression of desnutrin in 3T3-L1CARΔ1 adipocytes.

RESULTS—aP2-desnutrin mice were leaner with decreased adipose tissue TAG content and smaller adipocyte size. Overexpression of desnutrin increased lipolysis but did not result in increased serum nonesterified fatty acid levels or ectopic TAG storage. We found increased cycling between diacylglycerol (DAG) and TAG and increased fatty acid oxidation in adipocytes from these mice, as well as improved insulin sensitivity.

CONCLUSIONS—We show that by increasing lipolysis, desnutrin overexpression causes reduced adipocyte TAG content and attenuation of diet-induced obesity. Desnutrin-mediated lipolysis promotes fatty acid oxidation and re-esterification within adipocytes. ***Diabetes*** **58:855–866, 2009**

In mammals, white adipose tissue (WAT) is the primary energy storage depot, accumulating fuel reserves in the form of triacylglycerol (TAG) during times of energy excess (1). However, unlike TAG synthesis that also occurs at high levels in liver for VLDL production, lipolysis for the provision of fatty acids (FAs) as an energy source for use by other organs is unique to adipocytes. The release of FA from TAG proceeds in an orderly and regulated manner. TAG is hydrolyzed first to form diacylglycerol (DAG) and then monoacylglycerol (MAG) that is hydrolyzed to liberate the final FA and glycerol (1–4).

We and others have recently identified a TAG lipase that belongs to the patatin-like domain-containing family of proteins (5–7). We named this enzyme desnutrin (also called PNPLA2, adipose triglyceride lipase, TTS2.2, and iPLA$_2\zeta$) because it is induced during a low nutritional state in mice (i.e., fasting) and it belongs to the same patatin-like domain-containing family as another nutritionally regulated protein, adiponutrin. Desnutrin is highly expressed in adipose tissue but is also found at low levels in other tissues (6). Understanding the role of desnutrin in fat metabolism, specifically in adipose tissue, is of critical importance, because dysregulated adipocyte TAG lipolysis may cause elevated circulating FA concentrations that are associated with severe metabolic derangements, including the development of insulin resistance and type 2 diabetes (8). Central to this understanding is the question of the metabolic fate of FAs derived from desnutrin-mediated TAG lipolysis, particularly when the release of these FAs is dissociated from the energy requirements of other organs.

FAs liberated from adipocyte TAG can enter several possible metabolic pathways. Primarily, they are released to the systemic circulation, providing oxidative substrates for use by other tissues during energy deprivation and therefore maintaining whole-body energy homeostasis (1,9). Alternatively, however, FAs hydrolyzed from TAG can also be used directly within the adipocyte in re-esterification reactions producing TAG or other lipid species or in oxidative metabolism. FA oxidation occurs in the mitochondria and peroxisomes. Although mitochondrial FA oxidation is normally tightly coupled to ATP synthesis, uncoupling of this process can result in energy wasting and heat production. Peroxisomal FA oxidation is always poorly coupled, generating heat instead of ATP.

To investigate the adipocyte-specific function of desnutrin and the metabolic fate of FAs released from lipolysis, we generated transgenic mice constitutively overexpressing desnutrin in adipose tissue and also used adenoviral-mediated overexpression of desnutrin in differentiated 3T3-L1CARΔ1 adipocytes. We report that desnutrin-mediated lipolysis attenuates diet-induced obesity and, surprisingly, does not result in ectopic TAG storage or increased serum nonesterified FA (NEFA) levels. Rather, desnutrin overexpression increases apparent cycling between TAG and DAG (and/or MAG) in adipose tissue and promotes FA oxidation specifically within adipocytes. As a result, aP2-desnutrin mice are leaner and resistant to diet-induced obesity with improved insulin sensitivity.

RESEARCH DESIGN AND METHODS

Transgene construct and generation and maintenance of transgenic mice. The 1.7 kb coding sequence for hemagluttinin (HA)-tagged desnutrin, including a bovine growth hormone polyadenylation sequence, was subcloned under control of the 5.4-kb adipocyte FA-binding protein (aP2) promoter and microinjected into the pronucleus of fertilized eggs of C57BL/6 × CBA mice. aP2-desnutrin mice and their wild-type littermates were fed a high-fat diet (HFD) (45 kcal% fat, 35 kcal% carbohydrate, and 20 kcal% protein; Research

From the [1]Department of Nutritional Science and Toxicology, University of California, Berkeley, California; the [2]Department of Internal Medicine, Yale University, School of Medicine, New Haven, Connecticut and the [3]Department of Molecular and Cell Biology, University of California, Berkeley, California.

Corresponding author: Hei Sook Sul, hsul@nature.berkeley.edu.

Received 26 November 2008 and accepted 5 January 2009.

Published ahead of print at http://diabetes.diabetesjournals.org on 9 January 2009. DOI: 10.2337/db08-1644.

D.F. is currently affiliated with the Department of Physiology, School of Medicine of Ribeirao Preto, University of Sao Paulo, Sao Paulo, Brazil.

M.A. and R.E.D. contributed equally to this article.

Diets) ad libitum at weaning. Experiments were performed in 20-week-old transgenic mice and compared with sex-matched littermates.

RNA extraction and real-time RT-PCR. Total RNA was prepared using Trizol Reagent (Invitrogen), and cDNA was synthesized from 2.5 μg of total RNA by Superscript II reverse transcriptase (Invitrogen). Desnutrin-HA transgene expression was determined by RT-PCR (forward primer: 5′-CTACTGAACCAACCCAACCCT-3′; reverse primer: 5′-TTAGTAATCTGGAACATCGTATGGGTA-3′). Tissue gene expression was determined by RT-qPCR performed with an ABI PRISM 7700 sequence fast detection system (Applied Biosystems) and was quantified by measuring the threshold cycle normalized to glyceraldehyde-3-phosphate dehydrogenase (GAPDH) or β-actin and then expressed relative to wild-type controls.

Immunoblotting. Total lysates were subjected to 8% SDS-PAGE, transferred to PVDF membranes, and probed with rabbit anti-desnutrin antibody or rabbit anti-GAPDH antibody followed by peroxidase conjugated goat anti-rabbit antibody. Blots were visualized using enhanced chemiluminescence (PerkinElmer), and images were captured using a Kodak Image Station 4000MM.

Adipocyte size determination. Gonadal fat samples were fixed in 10% buffered formalin, embedded in paraffin, cut into 6-μm-thick sections, and stained with hematoxylin and eosin. Five separate fields from four different mice were quantified using a LEICA DM IRB microscope.

Ex vivo lipolysis. Gonadal fat pads from overnight-fasted mice were cut into 50-mg samples and incubated at 37°C in 500 μl of Krebs-Ringer medium buffered with bicarbonate plus HEPES containing 2% FA-free BSA and 0.1% glucose with or without 0.5 mmol/l dibutyryl cAMP (Sigma). FA and glycerol release were measured in aliquots from incubation buffer using the NEFA C Kit (Wako) and Free Glycerol Reagent (Sigma), respectively.

In vitro triolein lipase assay. TAG hydrolase activity of WAT extracts was performed essentially as described (10). Briefly, WAT was homogenized in lysis buffer (0.25 mol/l sucrose, 1 mmol/l EDTA, pH 7.0, 1 mmol/l DTT) and then centrifuged at 4°C for 20 min at 10,000*g*. Triolein lipase activity was assayed in 100 μg of supernatants. The reaction was initiated by addition of 100 μl of substrate that was prepared by sonicating 100 mmol/l potassium phosphate, 2 mmol/l EDTA, pH 7.4, with 200 μmol/l [^{3}H]triolein (40,000 cpm/reaction), 25 μmol/l lecithin, 10 μmol/l taurocholate, 1% BSA, and 1 mmol/l DTT. Reaction mixtures were incubated at 37°C for 30 min, terminated by addition of 3.25 ml of methanol/chloroform/heptane (10:9:7), and extracted with 1 ml of 0.1 mol/l potassium carbonate and 0.1 mol/l boric acid, pH 10.5. Liberated FAs were quantified in 700 μl of the upper phase by liquid scintillation counting.

Tissue analysis. Total neutral lipids were extracted by the method of Folch (11). Lipids were solubilized in 1% Triton X-100, and TAG was measured using Infinity Reagent (Thermo). Fat-free mass was estimated by subtracting total adipose tissue mass from body weights.

Cell culture. 3T3-CARΔ preadipocytes, provided by Dr. D. Orlicky (University of Colorado), were maintained and differentiated as previously described (12). These cells stably express the coxsackievirus and adenovirus receptor allowing for 100-fold greater transduction efficiency with adenovirus (13) but are otherwise indistinguishable from the parental 3T3-L1 cell line (14). For radiolipid studies, day 8 differentiated 3T3-CARΔ adipocytes grown in 12-well plates were pulse-labeled for 4 h with 0.05 μCi per well of [U-^{14}C]palmitic acid, washed with cold media, and infected at the start of the chase period at an MOI of ~100 with adenovirus expressing green fluorescent protein (GFP) or GFP-desnutrin. ^{14}C-FA was measured in the medium 30 h later by liquid scintillation. For studies on endogenous TAG content and lipolysis, adipocytes were infected as described at time point = 0. Three days later, medium was changed to serum-free medium, with or without dibutyryl cAMP, 6 h before measurement of FA and glycerol release. For imaging studies, 3T3-L1CARΔ adipocytes grown and differentiated on coverslips were stained with Nile Red and DAPI to visualize neutral lipids and nuclei, respectively, and were fixed for image capture using a Zeiss Axiophot LSM 510Meta confocal microscope. Total lipids were extracted from 3T3-L1CARΔ adipocytes by the method of Bligh and Dyer (15) and resolved by TLC in hexane:diethylether:acetic acid (80:20:2). For determination of endogenous lipids, the band corresponding to TAG was scraped and solubilized in 1% Triton X-100 and measured as described. Radiolabeled TAG was scraped and quantified by liquid scintillation counting.

Indirect calorimetry and body temperature. Oxygen consumption (V_{O_2}) was measured using the Comprehensive Laboratory Animal Monitoring System (Columbus Instruments). Data were normalized to body weights. Body temperatures were assessed in 25-week-old male mice using a RET-3 rectal probe for mice (Physitemp).

Hyperinsulinemic-euglycemic clamp. We implanted jugular venous catheters 7 days before the study. After an overnight fast, we infused [3-^{3}H]glucose (Perkin Elmer) at a rate of 0.05 μCi min^{-1} for 2 h to assess basal glucose turnover followed by the hyperinsulinemic-euglycemic clamp for 140 min with a primed/continuous infusion of human insulin (154 pmol/kg prime [21 mU/kg]) over 3 min followed by 17 pmol · kg^{-1} · min^{-1} (3 mU · kg^{-1} · min^{-1}) infusion (Novo Nordisk, Princeton, NJ), a continuous infusion of [3-^{3}H]glucose (0.1 μCi/min), and a variable infusion of 20% dextrose to maintain euglycemia (~100–120 mg/dl). We obtained plasma samples from the tail and measured tissue-specific glucose uptake after injection of a bolus of 10 μCi of 2-deoxy-D-[1-^{14}C]glucose (Perkin Elmer) at 85 min (16). We analyzed our results as previously described (17).

^2H_2O labeling and GCMS analysis of TAG-glycerol and TAG-FA. The heavy water (^2H_2O) labeling protocol and GCMS analyses of TAG-glycerol and TAG-FA from adipose tissue have been described previously in detail (18). Mice were administered ^2H_2O in drinking water starting at 20 weeks of age for a 2-week period after which lipids were extracted from gonadal fat pads by the method of Folch (11) for subsequent analysis.

Calculation of all-source TAG-glycerol synthesis. Fractional TAG-glycerol synthesized from α-glycerol phosphate during the period of ^2H_2O administration was measured as described (18):

$$f_{TAG} = EM1_{TAG\text{-}glycerol}/A_1\infty_{TAG\text{-}glycerol}.$$

EM1 is the measured excess mass isotopomer abundance for M_1-glycerol at time t and $A_1\infty$ is the asymptotic mass isotopomer abundance for M_1-glycerol, assuming that four of five C-H bonds of α-glycerol phosphate are replaced by H-atoms from tissue water (18).

Net lipolysis was estimated from f_{TAG} synthesis and adipose mass as follows:

$$[f_{TAG} \times (\text{adipose mass/labeling time}) - (\Delta\text{adipose mass/labeling time})]/\text{fat pad mass}.$$

Values with net lipolysis equivalent to zero were excluded from analysis.

Calculation of de novo lipogenesis. Fractional contributions from de novo lipogenesis (DNL) are calculated using a combinatorial model as previously described (18):

$$f_{DNL} = EM1_{FA}/A_1\infty_{FA}$$

where f_{DNL} represents the fraction of total TAG-palmitate in the depot that derived from DNL during the labeling period.

The fraction of newly synthesized TAG-palmitate that came from DNL is also calculated by correcting the measured fractional contribution from DNL (f_{DNL}) for the degree of replacement of adipose TAG during the labeling period:

$$\text{DNL contribution to newly synthesized TAG} = [f_{DNL}/f_{TAG}]$$

FA oxidation. Gonadal fat pads were digested for 1 h at 37°C with collagenase in Krebs-Ringer medium buffered with bicarbonate plus HEPES supplemented with 3 mmol/l glucose and 1% BSA, filtered through nylon mesh, and centrifuged, and adipocytes were collected from the upper phase. FA oxidation was determined by measuring $^{14}CO_2$ production from [^{14}C]palmitic acid (0.2 μCi/ml) after incubation for 1 h at 37°C with gentle shaking. The buffer was acidified with 0.25 ml of H_2SO_4 (5N) and maintained sealed at 37°C for an additional 30 min. Trapped radioactivity was quantified by liquid scintillation.

Serum parameters. Fasting serum triglycerides and FAs were analyzed with Infinity Triglyceride reagent (Thermo Trace) and NEFA C kit (Wako), respectively. Serum insulin, leptin, and adiponectin levels were determined using ELISA kits (Crystal Chem and B-Bridge).

The results are expressed as means ± SEM. Statistically significant differences between two groups were assessed by Student's *t* test. Differences between multiple groups were assessed by one-way ANOVA with Bonferroni's post hoc test.

RESULTS

Desnutrin overexpression in adipose tissue attenuates diet-induced obesity. We generated transgenic mice overexpressing HA-tagged desnutrin under control of the aP2 promoter to investigate the adipocyte-specific role of desnutrin. Results reported here are a comparison between mice from the founder line with the highest desnutrin transgene expression and their littermates. Similar results were obtained from an additional founder line (data not shown). RT-PCR analysis indicated that expression of the transgene was limited to WAT and brown adipose tissue (BAT) and was not detected in any other tissues examined (Fig. 1*A*). Desnutrin was expressed 4.8-fold and 3.4-fold above endogenous levels in gonadal

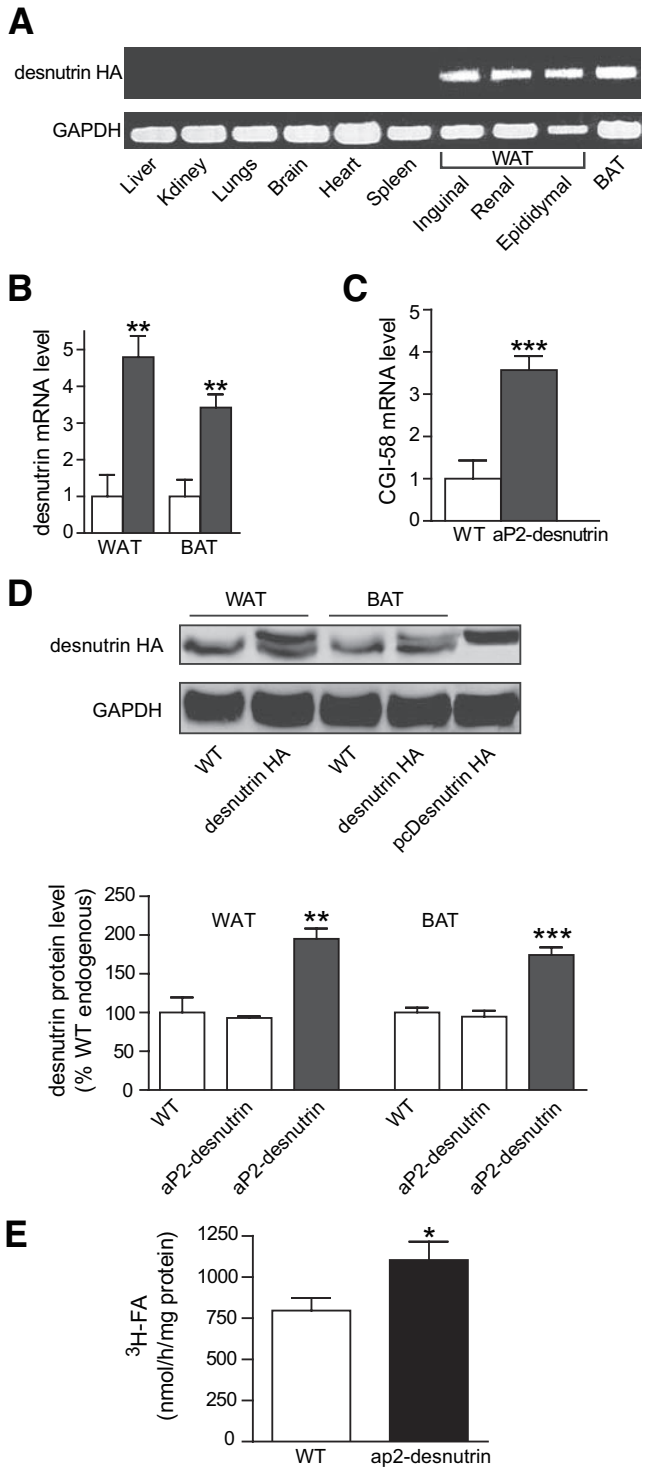

FIG. 1. Desnutrin overexpression in adipose tissue of mice. *A*: Transgene expression was verified by RT-PCR in tissues from aP2-desnutrin mice. GAPDH, glyceraldehyde-3-phosphate dehydrogenase. *B*: Desnutrin mRNA level in gonadal WAT and BAT as determined by RT-qPCR (n = 5–6). □, wild type; ■, aP2-desnutrin. *C*: CGI-58 mRNA level in gonadal WAT as determined by RT-qPCR (n = 6–7). *D*: Immunoblot and quantification of desnutrin-HA fusion protein in gonadal WAT and BAT. □, endogenous; ■, endogenous + transgene. *E*: TAG lipase activity in WAT homogenates from wild-type and aP2-desnutrin mice. *P < 0.05, **P < 0.01, ***P < 0.001. All data are from female mice. WT, wild type. (A high-quality digital representation of this figure is available in the online issue.)

WAT and BAT, respectively, as analyzed by RT-qPCR (Fig. 1*B*). We also detected a 3.5-fold increase in expression of CGI-58, a putative activator of desnutrin, in WAT of aP2-desnutrin mice (Fig. 1*C*). Using a desnutrin-specific antibody, we detected a band for desnutrin-HA protein in WAT and BAT of aP2-desnutrin mice but not in wild-type mice (Fig. 1*D*). We quantified desnutrin protein levels and found that although there was no difference in endogenous protein levels in both WAT and BAT in wild-type and aP2-desnutrin mice, total desnutrin levels (endogenous + transgene) were increased by approximately twofold in transgenic mice (Fig. 1*D*). To confirm the presence of a functional enzyme, we assayed homogenates of WAT from aP2-desnutrin mice and found a 40% increase in total triolein lipase activity (Fig. 1*E*). This represents a substantial increase in total triglyceride lipase activity over controls, because baseline TAG lipase activity is already considerable in WAT extracts as a result of the presence of additional triglyceride lipases, including hormone-sensitive lipase (1).

aP2-desnutrin mice and wild-type littermates were fed a standard chow diet or an HFD at weaning. On a chow diet, there was no difference in body weight (Fig. 2*B*, *inset*), fat pad weight, or organ weight between wild-type and aP2-desnutrin mice at 20 weeks of age (Fig. 2*C*, *left panels*). However, on an HFD, aP2-desnutrin mice were leaner (Fig. 2*A*, *upper panel*) and gained weight at a slower rate than wild-type littermates (Fig. 2*B*) despite similar food intakes (Fig. 2*A*, *lower panel*). Although there was no difference in kidney, lung, or heart weights, liver weights in aP2-desnutrin mice were 15% lower compared with wild type (Fig. 2*D*, *left panel*). Inguinal, gonadal, renal, and subcutaneous depots weighed 56, 59, 47, and 52% less, respectively, compared with depots from wild-type littermates (Fig. 2*D*, *right panel*). BAT depots from aP2-desnutrin mice weighed 20% less than depots from wild-type mice. We conclude that aP2-desnutrin mice are protected from HFD-induced obesity. To understand the mechanism underlying desnutrin-mediated protection from diet-induced obesity, we compared HFD-fed aP2-desnutrin mice and their wild-type littermates.

Decreased adipose tissue mass can result from a reduction in adipocyte size and/or a reduction in adipocyte number due to impaired differentiation (9,19–21). The expression level of adipocyte marker genes, including CCAAT/enhancer binding protein α (C/EBPα), preadipocyte factor (Pref)-1, peroxisome proliferator–activated receptor (PPAR)-γ, and aP2/a-FABP (adipocyte FA binding protein), was similar in aP2-desnutrin mice and their wild-type littermates on an HFD, suggesting normal adipocyte differentiation (Fig. 2*E*). Histological analysis, however, revealed a greater frequency of smaller adipocytes in gonadal fat pads from aP2-desnutrin mice when compared with wild-type littermates (Fig. 2*F*). We found a 55% reduction in adipose tissue TAG content in aP2-desnutrin mice relative to wild-type littermates (Fig. 3*A*), indicating that decreased adipocyte size and TAG content explains protection from diet-induced obesity. Because the effect of desnutrin on TAG stores has been shown only in nonadipocytes, which do not contain large lipid droplets (22), we also performed adenovirus-mediated overexpression of GFP-desnutrin in adipocytes (Fig. 3*B*). As previously shown (7), desnutrin localized strongly to lipid droplets in contrast to control GFP (Fig. 3*C*). Overexpression of desnutrin decreased endogenous TAG levels by 23% under basal conditions and by 25% after 6 h of stimulation with

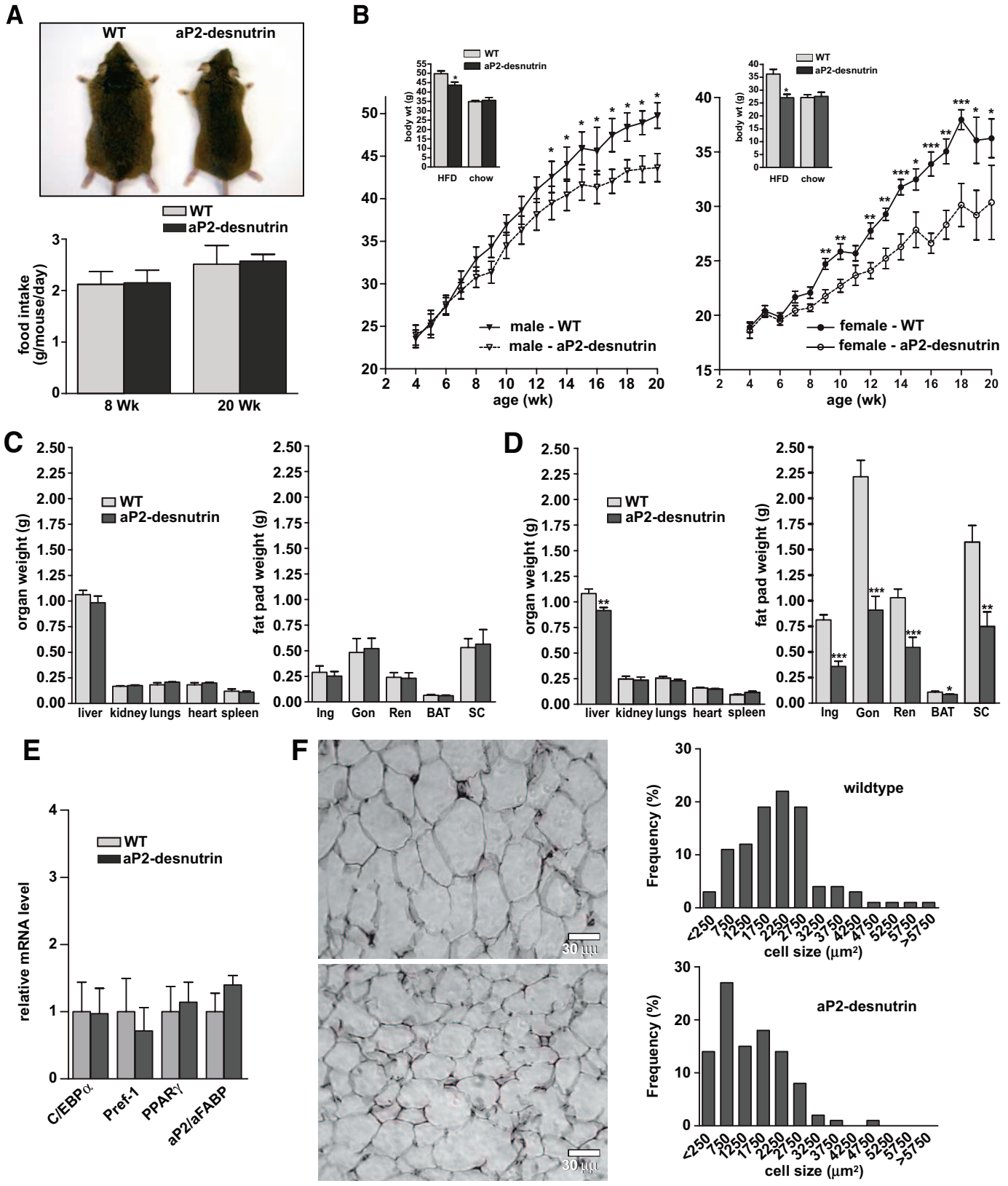

FIG. 2. Weight gain, fat pad weight, and adipocyte size in aP2-desnutrin mice. *A*: Gross appearance of female wild-type and aP2-desnutrin littermates (*upper panel*). Food intakes of female mice at 8 and 20 weeks (Wk) (*lower panel*). *B*: Time course of body weights over 20 weeks in mice fed an HFD. *Inset*: Average body weights at 20 weeks in mice fed a chow diet or an HFD (n = 9–11). *C* and *D*: Organ and fat pad weights in female mice fed a chow diet (*C*) or an HFD (*D*) (n = 9–11). Gon, gonadal fat pad; Ing, inguinal fat pad; Ren, renal fat pad; SC, subcutaneous fat pad. *E*: RT-qPCR for C/EBPα, Pref-1, PPARγ, and aP2/aFABP from WAT of female wild-type and aP2-desutrin mice fed an HFD (n = 4–6). *F*: Representative images of hematoxylin and eosin–stained sections of gonadal WAT and frequency distribution of adipocyte cell size in gonadal WAT. *P < 0.05, **P < 0.01, ***P < 0.001. (A high-quality digital representation of this figure is available in the online issue.)

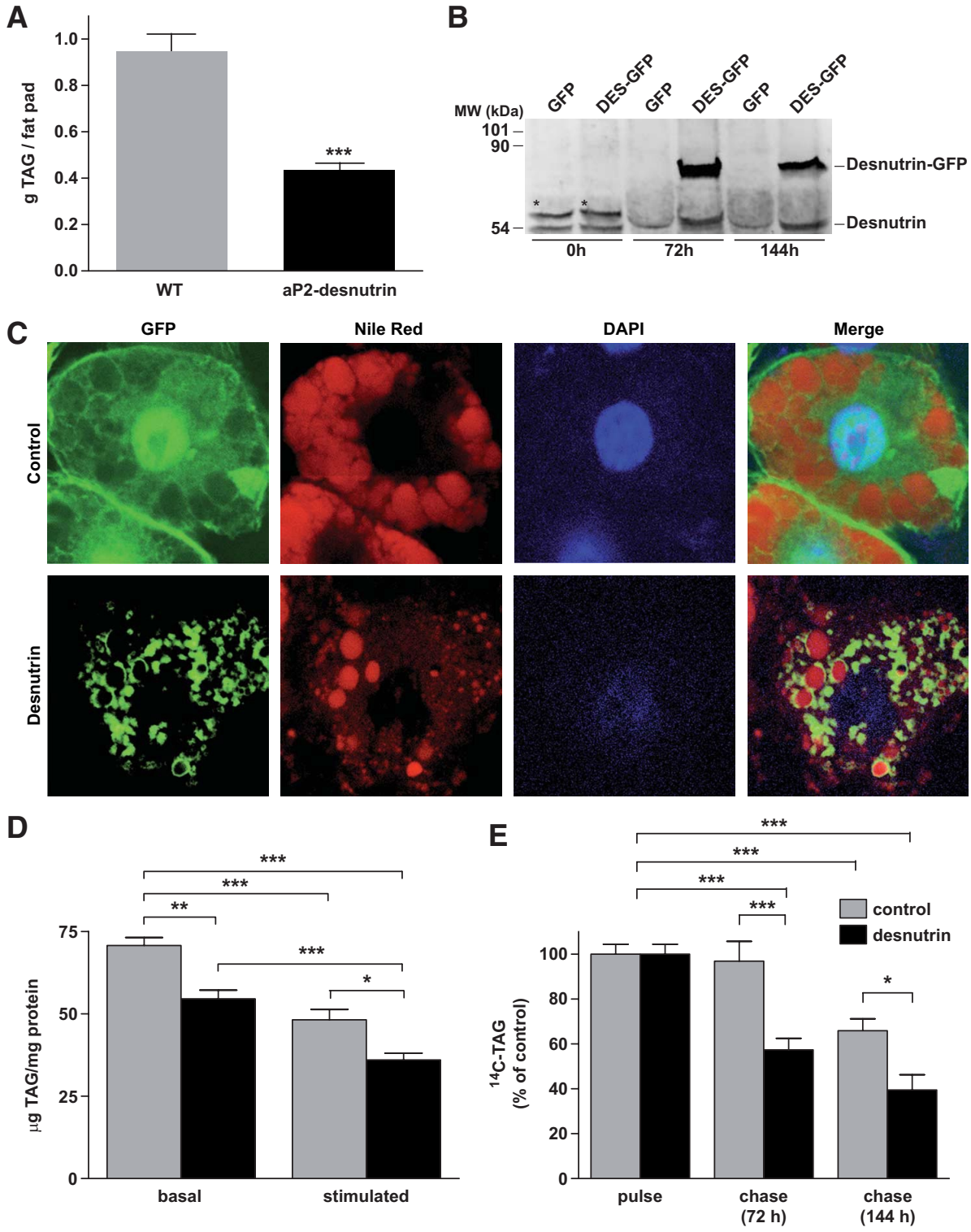

FIG. 3. Overexpression of desnutrin in adipocytes decreases TAG content. *A*: TAG content of gonadal fat pads (n = 6–9). WT, wild type. *B*: Immunoblot of endogenous desnutrin and desnutrin-GFP in differentiated 3T3-L1CARΔ1 adipocytes. *Nonspecific band. DES, desnutrin. *C*: Confocal microscopy images showing localization of desnutrin-GFP to TAG-rich lipid droplets in contrast to the diffuse localization of GFP alone. *D*: Endogenous TAG content from 3T3-L1CARΔ1 adipocytes. Three days after infection with GFP or desnutrin-GFP, medium was replaced with serum-free medium and cells were maintained for an additional 6 h either with dibutyryl cAMP (stimulated) or without (basal) before analysis of TAG content. *E*: Time course of TAG breakdown in 3T3-L1CARΔ1 adipocytes labeled with [^{14}C]palmitate before infection with GFP or desnutrin-GFP and chase with cold medium. *$P < 0.05$, **$P < 0.01$, ***$P < 0.001$. (A high-quality digital representation of this figure is available in the online issue.)

dibutyryl cAMP (Fig. 3*D*). Similarly, radiolabeled TAG was depleted more rapidly in cells overexpressing desnutrin-GFP than in cells expressing control GFP (Fig. 3*E*). Taken together, these results indicate that desnutrin overexpression results in smaller adipocytes with lower TAG content but does not affect differentiation.

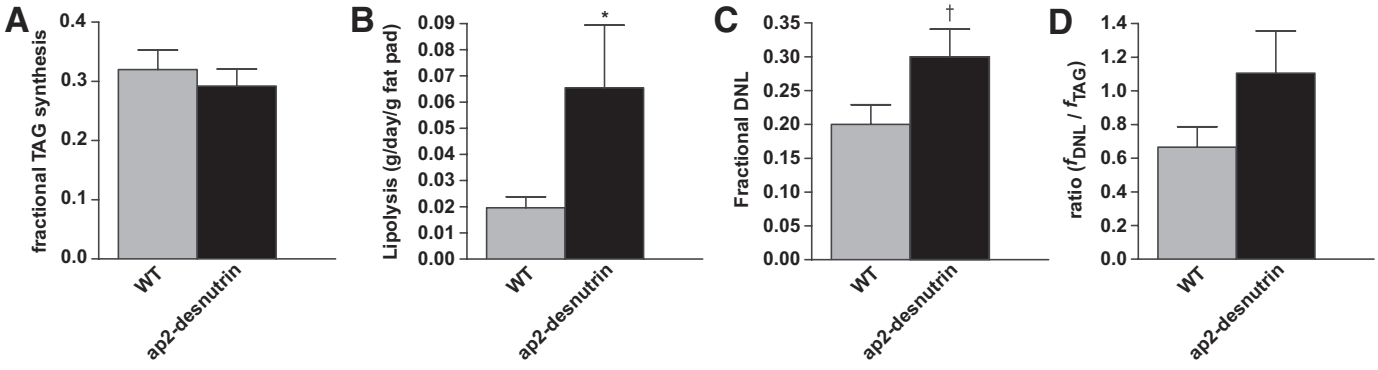

FIG. 4. In vivo measures of TAG metabolism in WAT. *A*: Fractional in vivo synthesis of TAG-glycerol in gonadal WAT ($n = 6$). *B*: In vivo lipolysis in gonadal WAT ($n = 3–6$). *C*: Fractional in vivo DNL in gonadal WAT ($n = 6$). *D*: Ratio of fractional in vivo DNL/fractional in vivo synthesis of TAG-glycerol in gonadal WAT ($n = 6$). *$P < 0.05$, †$P = 0.07$.

Desnutrin overexpression increases lipolysis and apparent cycling between TAG and DAG. We next measured in vivo TAG metabolism over a 2-week period using a recently developed heavy water labeling technique (18,23). The fractional contribution of TAG synthesis to adipose tissue TAG (f_{TAG}) was not different (Fig. 4*A*), although the net in vivo lipolytic rate, calculated from the absolute rate of new TAG synthesis and the change in adipose mass, was significantly higher per gram of adipose tissue in aP2-desnutrin mice compared with wild-type littermates (Fig. 4*B*). Interestingly, there was an increase ($P = 0.07$) in the fractional contribution from DNL (f_{DNL}) to adipose tissue palmitate in aP2-desnutrin mice compared with wild-type littermates (Fig. 4*C*). The ratio of de novo synthesized palmitate to new TAG synthesis (Fig. 4*D*), which represents the contribution from DNL to newly formed adipose TAG-palmitate (18,24), was greater than unity in aP2-desnutrin mice (1.10 ± 0.25) but less than unity in wild-type littermates (0.67 ± 0.12). This change in the ratio of DNL to TAG synthesis, particularly to values greater than 100%, in the absence of an increase in absolute DNL (data not shown), likely reflects recycling between TAG and DAG and/or MAG. This also suggests that re-esterification of DAG/MAG occurs predominantly with FA originating from DNL rather than from preexisting unlabeled FA. In support of our findings of increased re-esterification, we found no change in WAT DAG levels between wild-type and aP2-desnutrin mice (3.18 ± 0.32 μg/mg versus 3.26 ± 0.34 μg/mg, respectively). These results are consistent with increased TAG lipolysis in aP2-desnutrin mice, beyond that which was apparent from measures of the complete hydrolysis of TAG to free glycerol.

In agreement with our findings from in vivo lipolysis, we found that glycerol release from adipocytes isolated from fed aP2-desnutrin mice was significantly higher under basal and adenosine deaminase or isoproterenol-stimulated conditions (Fig. 5*A*, *left panel*). FA release was also significantly higher from adenosine deaminase or isoproterenol-treated adipocytes from aP2-desnutrin mice (Fig. 5*A*, *right panel*). We also found that FA release from explants of gonadal WAT incubated in the presence or absence of dibutyryl cAMP was 55% higher under basal conditions and 42% higher under dibutyryl cAMP-stimulated conditions after 4 h (Fig. 5*B*). Under basal conditions, glycerol release tended to be higher in explants from aP2-desnutrin mice compared with wild-type mice, although this difference did not reach significance (Fig. 5*C*). Under stimulated conditions, glycerol release was significantly higher in explants from aP2-desnutrin mice at both 2 h (65% higher) and 4 h (95% higher). Cultured 3T3-L1 adipocytes overexpressing desnutrin-GFP had a significantly increased release of FA (Fig. 5*D*) as well as glycerol (Fig. 5*E*), and the proportionate increase in the release of glycerol was greater under dibutyryl cAMP-stimulated conditions than under basal conditions (28% versus 12% higher, respectively).

aP2-desnutrin mice have improved insulin sensitivity. Because aP2-desnutrin mice have increased lipolysis and are protected from diet-induced obesity, we postulated there may be alterations in insulin sensitivity. To investigate insulin action on whole-body and tissue-specific glucose metabolism, we performed hyperinsulinemic–euglycemic clamps with radioisotope-labeled glucose infusion in HFD-fed wild-type and aP2-desnutrin mice. The steady-state glucose infusion rate during the clamps was higher in aP2-desnutrin mice, reflecting increased insulin responsiveness (Fig. 6*A–B*), and whole-body glucose uptake was increased by ~20% ($P < 0.08$) (Fig. 6*C*). Skeletal muscle 2-deoxyglucose uptake was 38% higher in aP2-desnutrin versus wild-type mice (Fig. 6*D*), whereas adipose tissue glucose uptake did not differ (Fig. 6*E*). The ability of insulin to suppress hepatic glucose production during the clamp was improved by 36% in aP2-desnutrin mice (Fig. 6*F*). Corresponding to increased hepatic insulin sensitivity, Oil red O staining of liver sections revealed smaller lipid droplets in aP2-desnutrin mice (Fig. 6*G*). We examined TAG levels in various nonadipose tissues and found significantly lower TAG levels in the livers of aP2-desnutrin mice and, although not statistically significant, a tendency toward lower TAG levels in other tissues, including skeletal muscle (Fig. *6H*). Despite increased lipolysis in aP2-desnutrin mice, we found no significant differences in most serum metabolites measured including NEFA and glycerol as well as TAG, adiponectin, and leptin (wild-type mice 5.77 ± 1.79 ng/ml versus aP2-desnutrin mice 3.73 ± 0.36 ng/ml, $n = 6$) (Table 1), although serum insulin levels were significantly lower in HFD-fed aP2-desnutrin mice (3.44 ± 0.27 ng/ml for wild-type versus 2.38 ± 0.16 ng/ml for aP2-desnutrin, $P < 0.01$).

Desnutrin overexpression increases thermogenesis, energy expenditure, and FA oxidation within adipose tissue. Because aP2-desnutrin mice had decreased adipose tissue mass but an equivalent intake of food and an absence of ectopic TAG storage compared with wild-type mice, we hypothesized that these mice may have increased energy expenditure. Average body temperatures measured over the course of a day were 0.28°C higher in aP2-

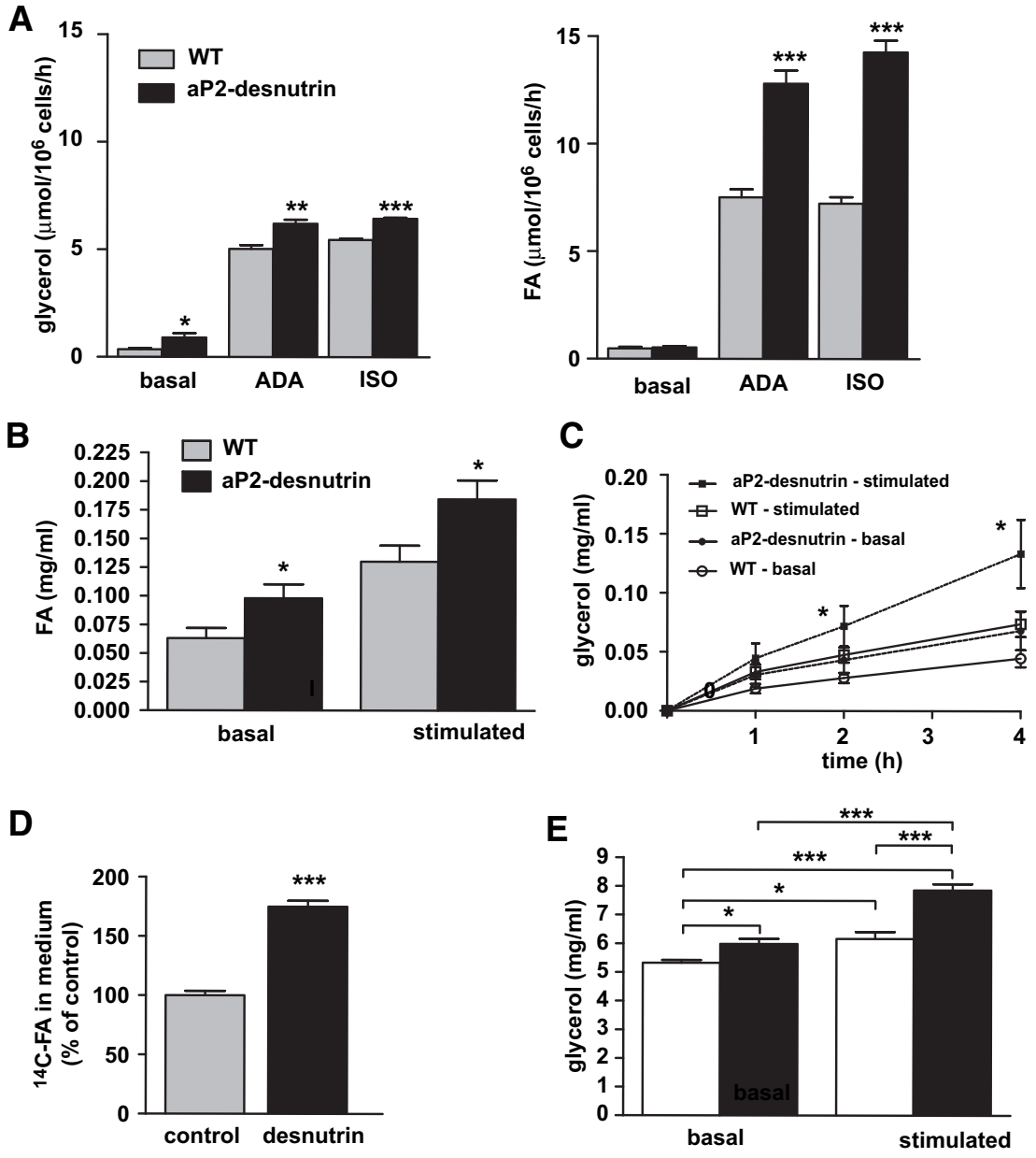

FIG. 5. Desnutrin overexpression increases lipolysis. *A*: Glycerol and FA release from isolated adipocytes of fed female wild-type or aP2-desnutrin mice under basal conditions or stimulated with adenosine deaminase (ADA) or isoproterenol (iso). FA (*B*) and glycerol (*C*) release from 50 mg explants of fresh gonadal WAT incubated under basal conditions or stimulated with 0.5 mmol/l dibutyryl cAMP (n = 9–12). *D*: Radiolabeled-FA release from 3T3-L1CARΔ1 adipocytes. Cells were labeled with [^{14}C]palmitate and then infected with adenoviral desnutrin-GFP or GFP (control) and chased with cold medium. [^{14}C]FA in the medium were quantified 30 h after infection. *E*: Glycerol release from 3T3-L1CARΔ1 adipocytes after infection with GFP or desnutrin-GFP for 3 days. Six hours before assessment of glycerol concentrations, medium was replaced with serum-free medium either with dibutyryl cAMP (stimulated) or without (basal). □, control; ■, desnutrin. *P < 0.05, **P < 0.01, ***P < 0.001. WT, wild type.

desnutrin compared with wild-type mice (Fig. 7*A*). To investigate the source of the increased thermogenesis, mice were housed in metabolic chambers for 24 h, where oxygen consumption and locomotor activity were assessed. Total oxygen consumption was 30% higher in aP2-desnutrin mice over a 24-h period (Fig. 7*B*). Activity levels, however, were not different between aP2-desnutrin and wild-type mice (data not shown). Thus, aP2-desnutrin mice have increased energy expenditure without changes in food intake or physical activity.

To further investigate potential mechanisms underlying the increased thermogenesis and oxygen consumption in aP2-desnutrin mice, we examined genes involved in oxidative metabolism. In skeletal muscle and liver, two tissues that play an important role in the use and regulation of energy substrates, there were no significant differences in the expression of acyl CoA oxidase or PPARα between wild-type and aP2-desnutrin mice (Fig. 8*C* and *D*). In BAT of aP2-desnutrin mice, uncoupling protein (UCP)-1 was upregulated by 2.9-fold (Fig. 8*B*). PPARγ coactivator (PGC)-1α was also upregulated by 4.2-fold in BAT of aP2-desnutrin mice. However, the significance of the changes in expression of these genes in BAT is unclear because we observed no difference in cold tolerance when mice were housed at an ambient temperature of 4°C (data not shown). However, there was a significant upregulation in aP2-desnutrin WAT of genes involved in thermogenesis and in both mitochondrial and peroxisomal FA oxidation

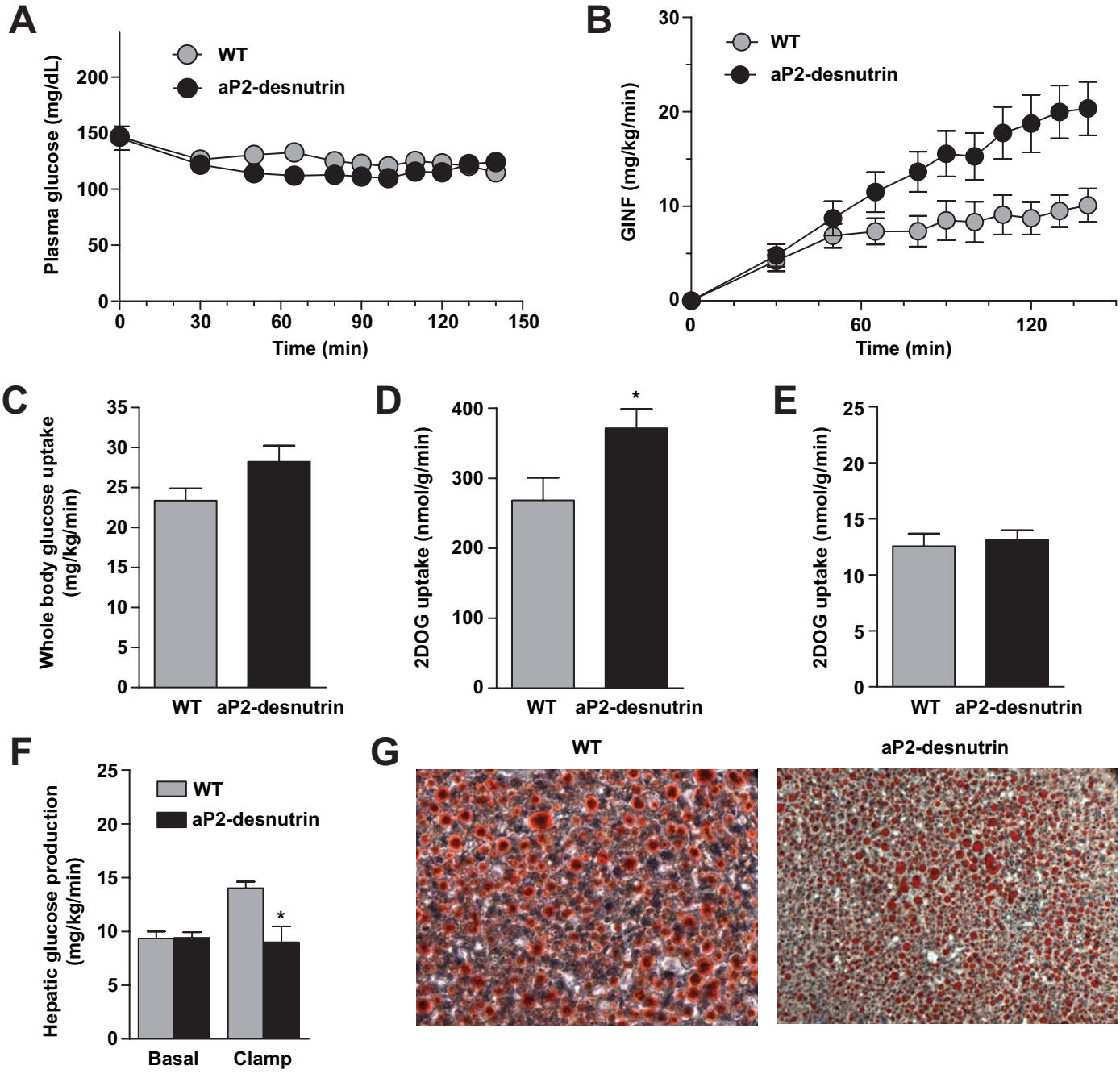

H

	μ g TAG/mg tissue		
Tissue	WT	aP2-desnutrin	*P* value
Liver	181.5 ± 18.0	102.2 ± 27.4	0.03
Skeletal muscle	3.9 ± 0.8	3.2 ± 0.4	0.76
Kidney	18.7 ± 4.6	12.6 ± 3.5	0.31
Heart	7.3 ± 2.9	11.3 ± 2.9	0.41
Spleen	4.2 ± 1.2	3.8 ± 1.0	0.79
Lungs	36.6 ± 18.4	17.8 ± 5.6	0.37
Brain	2.7 ± 1.0	3.2 ± 0.9	0.71

FIG. 6. Improved insulin sensitivity in aP2-desnutrin mice. *A* and *B*: Plasma glucose (*A*) and glucose infusion (GINF) (*B*) rates (n = 7–8) *C*: Whole-body glucose uptake (n = 7–8). *D*: Skeletal muscle (gastrocnemius) glucose uptake (n = 7–8). *E*: Epididymal WAT glucose uptake (n = 7–8). *F*: Hepatic glucose production during hyperinsulinemic-euglycemic clamps (n = 7–8). *G*: Cryosections of frozen livers stained with Oil red O. *H*: Tissue TAG content in indicated organs (n = 3–9). *$P < 0.05$. (A high-quality digital representation of this figure is available in the online issue.)

TABLE 1
Serum parameters of chow- or HFD-fed and fasted male mice

	Chow				HFD			
	Wild-type fasted	aP2-des fasted	Wild-type fed	aP2-des fed	Wild-type fasted	aP2-des fasted	Wild-type fed	aP2-des fed
FA (mmol/l)	1.57 ± 0.09	1.86 ± 0.10	0.84 ± 0.06	1.00 ± 0.07	1.39 ± 0.06	1.46 ± 0.11	0.84 ± 0.07	1.00 ± 0.07
Glycerol (mmol/l)	0.76 ± 0.02	0.82 ± 0.04	0.65 ± 0.04	0.66 ± 0.02	0.76 ± 0.03	0.72 ± 0.03	0.66 ± 0.02	0.76 ± 0.05
Triglyceride (mg/dl)	69.81 ± 1.50	67.55 ± 3.63	74.46 ± 4.17	76.33 ± 3.30	70.65 ± 3.06	65.34 ± 1.68	61.21 ± 2.46	65.71 ± 5.07
Adiponectin (μg/ml)	14.75 ± 1.08	15.10 ± 0.83	—	—	17.05 ± 0.79	17.35 ± 0.80	—	—

(Fig. 8*A*), including UCP-1 (7.1-fold), carnitine palmitoyltransferase (CPT)-1β (3.7-fold), PPARα (3.4-fold), PPARδ (2.4-fold), PGC-1α (3.3-fold), fatty acyl coA oxidase (AOx) (4.4-fold), phytanoyl-CoA hydroxylase (PhyH) (2.4-fold), and catalase (4.4-fold). When we measured the production of $^{14}CO_2$ from [^{14}C]palmitate in isolated adipocytes, we found that it was almost 2.5-fold higher in WAT of aP2-desnutrin mice compared with their wild-type littermates (Fig. 8*E*), clearly demonstrating increased FA oxidation within adipocytes from aP2-desnutrin mice. Therefore, in agreement with our observation that serum NEFA is unchanged in aP2-desnutrin mice, we report that desnutrin overexpression increases expression of oxidative genes and promotes FA oxidation in adipocytes.

DISCUSSION

Dysregulation of adipocyte lipolysis, resulting in elevated circulating NEFA, is associated with obesity and comorbidities, including the development of type 2 diabetes (8). Understanding the effects of desnutrin overexpression on adipose tissue TAG hydrolysis and TAG stores, as well as subsequent FA metabolism is therefore fundamental to the investigation of obesity and obesity-related diseases. Using transgenic mice constitutively overexpressing desnutrin in adipose tissue as well as adenoviral-mediated overexpression of desnutrin in differentiated 3T3-L1CARΔ1 adipocytes, we investigated the metabolic fate of FA derived from desnutrin-mediated TAG lipolysis.

Mice lacking desnutrin showed accumulation of TAG in a variety of tissues with a relatively small (approximately twofold) increase in WAT mass and premature mortality with massive TAG accumulation in the heart (25). We show that desnutrin overexpression in adipose tissue of mice attenuated diet-induced obesity by reducing fat pad TAG content and adipocyte size. Desnutrin overexpression in differentiated 3T3-L1CARΔ1 adipocytes also resulted in accelerated TAG breakdown, causing depletion of TAG stores. Our results from aP2-desnutrin mice are in contrast to results from a previous study in which adipose tissue overexpression of hormone-sensitive lipase did not result in a leaner phenotype in mice fed an HFD (26). New insights into the metabolic fate of FA generated from TAG were provided by the in vivo heavy water labeling study. The net in vivo lipolytic rate over 2 weeks, which represents the complete turnover of TAG to glycerol and FA, was elevated in adipose tissue from aP2-desnutrin mice. Findings were also consistent with increased re-esterification of DAG (and/or MAG) to TAG predominantly with newly synthesized FAs and suggested that although desnutrin overexpression increased the hydrolysis of TAG to DAG, a major fate of that DAG was retention within adipocytes. This finding also suggests that TAG lipolysis to DAG occurred at an even greater rate than that which is apparent from measures of the complete hydrolysis of TAG to free glycerol.

Despite the marked increase in lipolysis in adipose tissue of aP2-desnutrin mice, serum NEFA levels were not increased. FA levels in the blood represent a balance between liberation from adipose tissue and uptake by peripheral tissues, and therefore a number of factors may play a role in regulating serum NEFA concentrations. Net FA liberation is likely lower than expected in aP2-desnutrin mice, because adipose tissue mass is substantially reduced compared with wild-type mice. Increased removal of FA from the bloodstream by other organs may also have contributed, although TAG content was not increased in any tissues measured and was, in fact, significantly decreased in livers of aP2-desnutrin mice. Results from our heavy water labeling study suggest that, at least in part, increased re-esterification may have limited the release of FAs from adipose tissue in vivo. However, because re-esterification appeared to involve the incorporation of newly synthesized FAs to a greater extent than preexisting fatty acids, and because aP2-desnutrin mice had reduced adipose TAG content, increased loss of the hydrolyzed FA from adipose tissue was also indicated. Although there was no change in oxidative gene expression in skeletal muscle or liver, there was a substantial upregulation in aP2-desnutrin WAT of genes involved in mitochondrial β-oxidation such as CPT-1β; in peroxisomal α-oxidation such as AOx, PhyH, and catalase; and in thermogenesis such as PPARα, PPARδ, and PGC-1α. The most striking change was a 7.1-fold upregulation of UCP-1 expression. Measurement of FA oxidation by adipocytes isolated from aP2-desnutrin mice indicated a marked increase compared with their wild-type littermates and confirmed increased use of FAs directly within adipose tissue. Notably, UCP-1 induction results in increased heat production at the expense of ATP synthesis, as does peroxisomal FA α-oxidation, and aP2-desnutrin mice had significantly higher body temperatures over the course of the day, corresponding to a significantly higher rate of oxygen consumption. Taken together, our findings indicate that increased thermogenesis resulting from oxidation of hydrolyzed FAs within adipose tissue of aP2-desnutrin mice contributed to the leaner phenotype and, at least in part, to the absence of a rise in serum NEFA in these mice.

Although the present study is the first to demonstrate regulation of FA oxidation after overexpression of a TAG lipase, others have suggested that increased oxidation in adipocytes may contribute to protection against the development of diet-induced obesity (27–29). For example, overexpression of UCP-1 in WAT of mice has been shown to increase respiratory uncoupling specifically in WAT, resulting in a leaner phenotype (27), and hyperleptinemia in rats was found to increase WAT UCP-1 and adipocyte FA oxidation, resulting in dramatic fat loss (28). Perilipin null mice also have elevated adipocyte FA oxidation and a

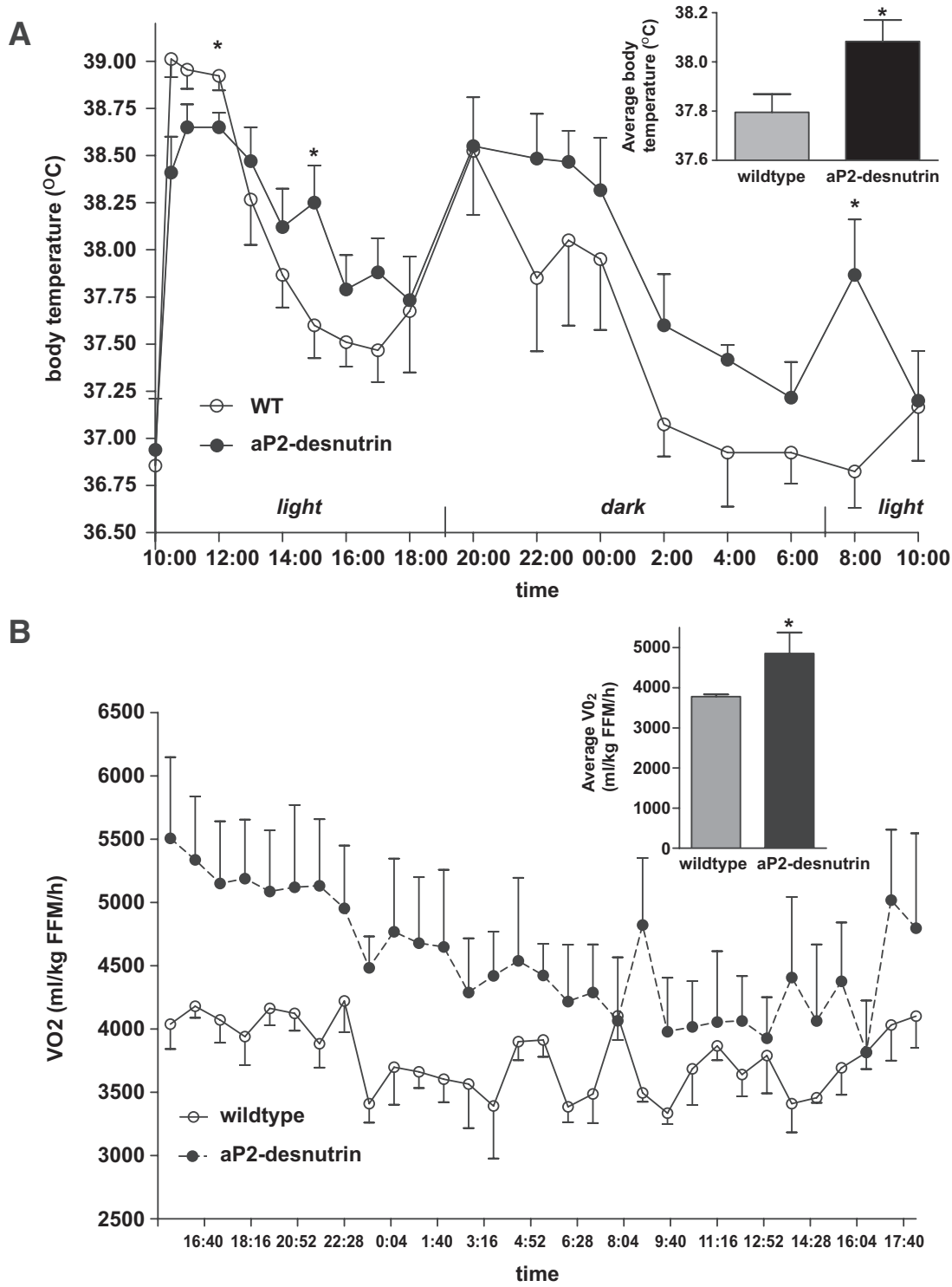

FIG. 7. Increased thermogenesis and energy expenditure in aP2-desnutrin mice. *A*: Body temperatures of 20-week-old male mice. Temperatures were measured beginning at 10 AM following a 17-h overnight fast and before resumption of feeding and were monitored for 24 h ($n = 4–6$). *Inset*: Average body temperature (°C) over the day. *B*: Oxygen consumption rate (V_{O_2}) measured through indirect calorimetry and the average V_{O_2} over 24 h (*inset*) ($n = 4$). *$P < 0.05$. FFM, fat-free mass.

leaner phenotype (27–29). These studies support our finding of leanness in aP2-desnutrin mice that have increased UCP-1 expression and adipocyte FA oxidation.

In association with their leaner phenotype, aP2-desnutrin mice demonstrate improved insulin sensitivity in hyperinsulinemic-euglycemic clamping studies attributable primarily to increased insulin-stimulated skeletal muscle glucose uptake and suppression of hepatic glucose production. Decreased liver TAG content may have contributed to the improved hepatic insulin sensitivity in these mice. Despite abundant evidence of increased lipolysis in aP2-desnutrin mice, circulating NEFA levels were unchanged and therefore cannot be a factor in mediating changes in insulin sensitivity. Adiponectin and leptin levels, which are associated with insulin sensitivity, were also unchanged in these mice. Thus, our aP2-desnutrin mice

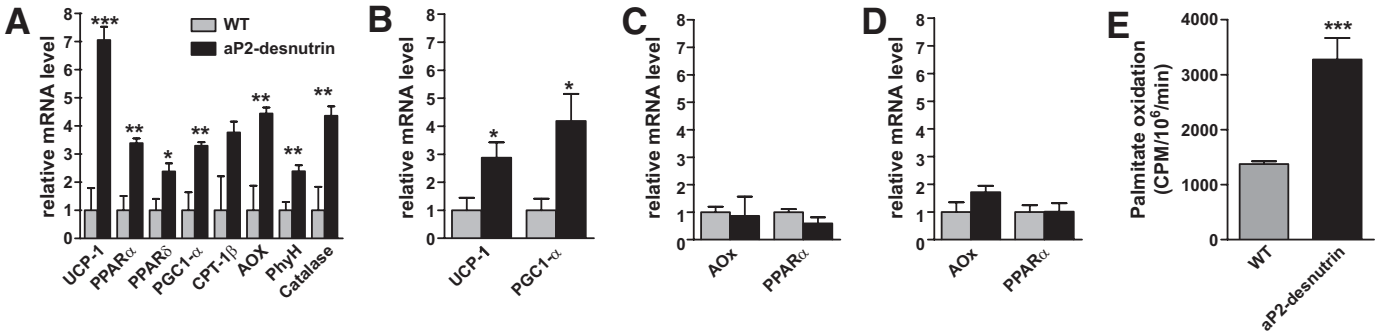

FIG. 8. Gene expression in WAT, BAT, liver, and skeletal muscle and increased FA oxidation in adipocytes. Relative mRNA levels were measured by RT-qPCR for the indicated genes from WAT (*A*), BAT (*B*), liver (*C*), and skeletal muscle (*D*) ($n = 5–6$). *E*: Oxidation of [^{14}C]palmitate to $^{14}CO_2$ by adipocytes isolated from aP2-desnutrin mice or wild-type (WT) controls. WT, light gray bars; aP2-desnutrin, black bars. *$P < 0.05$, **$P < 0.01$, ***$P < 0.001$. AOx, α-oxidation.

represent a new model in which a long-term increase in adipocyte lipolysis results in metabolic adaptations, including increased FA oxidation, leanness, and improved insulin sensitivity. In this regard, mice overexpressing UCP-1 in adipose tissue also exhibit leanness and increased adipocyte FA oxidation (27), as well as an unexplained improvement in insulin sensitivity (30). Given the similarities of the two models, it is possible that investigation of yet to be identified factors linking increased energy use in WAT to insulin sensitivity may provide new insight into understanding obesity/diabetes.

In conclusion, we show that, by increasing lipolysis, overexpression of desnutrin in adipose tissue causes reduced adipocyte TAG content and attenuation of diet-induced obesity, at least in part, by promoting FA oxidation and re-esterification within adipocytes. Overexpression of desnutrin in adipocytes also causes improved insulin responsiveness resulting from increased peripheral and hepatic insulin sensitivity that occurs independent of changes in circulating NEFA levels.

ACKNOWLEDGMENTS

This work was supported in part by DK75682 from the National Institutes of Health (NIH) to H.S.S., by MMPC (U24 DK59635) from the NIH to G.S., and by a grant to M.K.H. from the College of Natural Resources, University of California at Berkeley. R.E.D. and K.A.V. are recipients of postdoctoral fellowships from the Natural Sciences and Engineering Research Council of Canada. R.E.D. is a recipient of a postdoctoral fellowship from the Canadian Institutes of Health Research. D.F. is a recipient of a doctoral fellowship from The State of Sao Paulo Research Foundation (FAPESP 05/54620-3). A.L.B is a recipient of a postdoctoral fellowship from the Deutsche Forschungsgemeinschaft (German Research Foundation).

No potential conflicts of interest relevant to this article were reported.

We thank Matthew Bruss for insightful discussion and Jenny Chen, Ruzly Mantara, Jennifer Lu, Chris Lange, and James V. Chithalen for assistance.

REFERENCES

1. Duncan RE, Ahmadian M, Jaworski K, Sarkadi-Nagy E, Sul HS: Regulation of lipolysis in adipocytes. *Annu Rev Nutr* 27:79–101, 2007
2. Chon S-H, Zhou YX, Dixon JL, Storch J: Developmental and nutritional regulation of monoacylglycerol lipase and monoacylglycerol acyltransferase. *J Biol Chem* 282:33346–33357, 2007
3. Jaworski K, Sarkadi-Nagy E, Duncan RE, Ahmadian M, Sul HS: Regulation of triglyceride metabolism. IV. Hormonal regulation of lipolysis in adipose tissue. *Am J Physiol Gastrointest Liver Physiol* 293:G1–G4, 2007
4. Tornqvist H, Belfrage P: Purification and some properties of a monoacylglycerol-hydrolyzing enzyme of rat adipose tissue. *J Biol Chem* 251:813–819, 1976
5. Jenkins CM, Mancuso DJ, Yan W, Sims HF, Gibson B, Gross RW: Identification, cloning, expression, and purification of three novel human calcium-independent phospholipase A2 family members possessing triacylglycerol lipase and acylglycerol transacylase activities. *J Biol Chem* 279:48968–48975, 2004
6. Villena JA, Roy S, Sarkadi-Nagy E, Kim KH, Sul HS: Desnutrin, an adipocyte gene encoding a novel patatin domain-containing protein, is induced by fasting and glucocorticoids: ectopic expression of desnutrin increases triglyceride hydrolysis. *J Biol Chem* 279:47066–47075, 2004
7. Zimmermann R, Strauss JG, Haemmerle G, Schoiswohl G, Birner-Gruenberger R, Riederer M, Lass A, Neuberger G, Eisenhaber F, Hermetter A, Zechner R: Fat mobilization in adipose tissue is promoted by adipose triglyceride lipase. *Science* 306:1383–1386, 2004
8. Unger RH: Lipotoxic diseases. *Annu Rev Med* 53:319–336, 2002
9. Gregoire FM, Smas CM, Sul HS: Understanding adipocyte differentiation. *Physiol Rev* 78:783–809, 1998
10. Soni KG, Lehner R, Metalnikov P, O'Donnell P, Semache M, Gao W, Ashman K, Pshezhetsky AV, Mitchell GA: Carboxylesterase 3 (EC 3.1.1.1) is a major adipocyte lipase. *J Biol Chem* 279:40683–40689, 2004
11. Folch J, Lees M, Sloane Stanley GH: A simple method for the isolation and purification of total lipides from animal tissues. *J Biol Chem* 226:497–509, 1957
12. Kim KH, Lee K, Moon YS, Sul HS: A cysteine-rich adipose tissue-specific secretory factor inhibits adipocyte differentiation. *J Biol Chem* 276:11252–11256, 2001
13. Orlicky DJ, DeGregori J, Schaack J: Construction of stable coxsackievirus and adenovirus receptor-expressing 3T3–L1 cells. *J Lipid Res* 42:910–915, 2001
14. Ross SA, Song X, Burney MW, Kasai Y, Orlicky DJ: Efficient adenovirus transduction of 3T3–L1 adipocytes stably expressing coxsackie-adenovirus receptor. *Biochem Biophys Res Commun* 302:354–358, 2003
15. Bligh EG, Dyer WJ: A rapid method of total lipid extraction and purification. *Can J Biochem Physiol* 37:911–917, 1959
16. Youn JH, Buchanan TA: Fasting does not impair insulin-stimulated glucose uptake but alters intracellular glucose metabolism in conscious rats. *Diabetes* 42:757–763, 1993
17. Samuel VT, Choi CS, Phillips TG, Romanelli AJ, Geisler JG, Bhanot S, McKay R, Monia B, Shutter JR, Lindberg RA, Shulman GI, Veniant MM: Targeting foxo1 in mice using antisense oligonucleotides improves hepatic and peripheral insulin action. *Diabetes* 55:2042–2050, 2006
18. Turner SM, Murphy EJ, Neese RA, Antelo F, Thomas T, Agarwal A, Go C, Hellerstein MK: Measurement of TG synthesis and turnover in vivo by 2H2O incorporation into the glycerol moiety and application of MIDA. *Am J Physiol Endocrinol Metab* 285:E790–E803, 2003
19. Lee K, Villena JA, Moon YS, Kim K-H, Lee S, Kang C, Sul HS: Inhibition of adipogenesis and development of glucose intolerance by soluble preadipocyte factor-1 (Pref-1). *J Clin Invest* 111:453–461, 2003
20. Smas CM, Sul HS: Pref-1, a protein containing EGF-like repeats, inhibits adipocyte differentiation. *Cell* 73:725–734, 1993

21. Villena JA, Kim K-H, Sul HS: Pref-1 and ADSF/resistin: two secreted factors inhibiting adipose tissue development. *Horm Metab Res* 34:1–7, 2002
22. Smirnova E, Goldberg EB, Makarova KS, Lin L, Brown WJ, Jackson CL: ATGL has a key role in lipid droplet/adiposome degradation in mammalian cells. *EMBO Rep* 7:106–113, 2006
23. Turner SM, Roy S, Sul HS, Neese RA, Murphy EJ, Samandi W, Roohk DJ, Hellerstein MK: Dissociation between adipose tissue fluxes and lipogenic gene expression in ob/ob mice. *Am J Physiol Endocrinol Metab* 292: E1101–E1109, 2007
24. Strawford A, Antelo F, Christiansen M, Hellerstein MK: Adipose tissue triglyceride turnover, de novo lipogenesis, and cell proliferation in humans measured with 2H20. *Am J Physiol Endocrinol Metab* 286:E577–E588, 2003
25. Haemmerle G, Lass A, Zimmermann R, Gorkiewicz G, Meyer C, Rozman J, Heldmaier G, Maier R, Theussl C, Eder S, Kratky D, Wagner EF, Klingenspor M, Hoefler G, Zechner R: Defective lipolysis and altered energy metabolism in mice lacking adipose triglyceride lipase. *Science* 312:734–737, 2006
26. Lucas S, Tavernier G, Tiraby C, Mairal A, Langin D: Expression of human hormone-sensitive lipase in white adipose tissue of transgenic mice increases lipase activity but does not enhance in vitro lipolysis. *J Lipid Res* 44:154–163, 2003
27. Kopecky J, Clarke G, Enerback S, Spiegelman B, Kozak LP: Expression of the mitochondrial uncoupling protein gene from the aP2 gene promoter prevents genetic obesity. *J Clin Invest* 96:2914–923, 1995
28. Orci L, Cook WS, Ravazzola M, Wang M, Park BH, Montesano R, Unger RH: Rapid transformation of white adipocytes into fat-oxidizing machines. *Proc Natl Acad Sci U S A* 101:2058–2063, 2004
29. Saha PK, Kojima H, Martinez-Botas J, Sunehag AL, Chan L: Metabolic adaptations in the absence of perilipin. *J Biol Chem* 279:35150–35158, 2004
30. Yamada T, Katagiri H, Ishigaki Y, Ogihara T, Imai J, Uno K, Hasegawa Y, Gao J, Ishihara H, Niijima A, Mano H, Aburatani H, Asano T, Oka Y: Signals from intra-abdominal fat modulate insulin and leptin sensitivity through different mechanisms: neuronal involvement in food-intake regulation. *Cell Metab* 3:223–229, 2006